

# Pressure induced quenching of planar rattling in $\text{Cu}_{10}\text{Zn}_2\text{Sb}_4\text{S}_{13}$ studied by specific-heat and x-ray diffraction measurements

Kazunori Umeo,<sup>1,\*</sup> Koichiro Suekuni,<sup>2</sup> Toshiro Takabatake,<sup>3</sup> and Eiji Nishibori<sup>4</sup>

<sup>1</sup>*Department of Low Temperature Experiment,  
Integrated Experimental Support / Research Division, N-BARD,  
Hiroshima University, Higashi-Hiroshima, 739-8526, Japan*

<sup>2</sup>*Department of Applied Science for Electronics and Materials,  
Interdisciplinary Graduate School of Engineering Sciences,  
Kyushu University, Fukuoka 816-8580, Japan*

<sup>3</sup>*Graduate School of Advanced Science and Engineering,  
Hiroshima University, Higashi-Hiroshima 739-0826, Japan*

<sup>4</sup>*Department of Physics, Faculty of Pure and Applied Sciences,  
and Tsukuba Research Center for Energy Materials Science (TREMS),  
University of Tsukuba, 1-1-1 Tennodai Tsukuba, Ibaraki, 305-8571, Japan*

(Dated: April 10, 2024)

## Abstract

We have studied the pressure effect on the rattling of tetrahedrite  $\text{Cu}_{10}\text{Zn}_2\text{Sb}_4\text{S}_{13}$  (CZSS) and type-I clathrate  $\text{Ba}_8\text{Ga}_{16}\text{Sn}_{30}$  (BGS) by specific heat and x-ray diffraction measurements. By applying pressure  $P$ , the rattling energy for CZSS initially decreases and steeply increases for  $P > 1$  GPa. By contrast, the energy for BGS increases monotonically with  $P$  up to 6.5 GPa. An analysis of the pressure dependent specific heat and x-ray diffraction indicates that the out-of-plane rattling of the Cu atoms in the  $\text{S}_3$  triangle of CZSS originates from the chemical pressure, unlike the rattling of the Ba ions among off-center sites in an oversized cage of BGS. The rattling in CZSS ceases upon further increasing  $P$  above 2 GPa, suggesting that Cu atoms escape away from the  $\text{S}_3$  triangle plane.

Localized vibrational states of atoms in solids are attracting much attention in the fields of solid state physics and materials science [1, 2]. Such states are realized in compounds with a three-dimensional network of polyhedral cages including one guest atom. When the cage is oversized compared to the guest atom, so called “rattling modes” can be realized [3]. This concept was introduced by Slack to describe the situation where the guest atom moves among two or more semistable positions and no long-range correlation exists between their positions or orientations [3]. The rattling modes give rise to unusual physical properties: a strong suppression of the lattice thermal conductivity  $\kappa_L$  in some type-I clathrates  $X_8\text{Ga}_{16}\text{Ge}_{30}$  ( $X = \text{Eu}, \text{Sr}$ ) and  $\text{Ba}_8\text{Ga}_{16}\text{Sn}_{30}$  (BGS) [4, 5], and superconductivity in  $\beta$ -pyrochlore oxides  $\text{AOs}_2\text{O}_6$  ( $A = \text{K}, \text{Rb}, \text{Cs}$ ) [6] and  $\text{VAl}_{10.1}$  [7]. Because low  $\kappa_L$  is one of the requisites for thermoelectric materials, a number of experimental and theoretical works have been conducted to clarify how the rattling scatters acoustic phonons [2, 8].

Rattling vibrations in caged compounds depend on the difference between the cage size and the guest size [2]. When the cage size is reduced by applying pressure or by substituting the cage atoms with smaller ones, it is expected that the rattling energy is increased and the anharmonicity in the vibrational mode is weakened. Among clathrates, one of the well-studied examples is BGS, where the Ba guest atom exhibits so-called off-center rattling in a tetrakaidekahedral cage consisting of Ga and Sn atoms [5, 9]. When the cage of BGS is pressurized up to 6 GPa at room temperature, the guest atom moves from an off-center to on-center position and the energy of the rattling vibration increases, as found by high-pressure Raman scattering experiments [10]. When the cage size of  $\text{Sr}_8\text{Ga}_{16}\text{Ge}_{30}$  is decreased by the substitution of Si for Ge, the rattling energy is also enhanced, as found by specific-heat measurements [11].

Recently, rattling phenomena have been found even in non-caged compounds in which a rattling atom has a planar coordination. For example, large amplitude out-ofplane motion, which is called “planar rattling” [12], occurs for Bi atoms in  $\text{LaOBiS}_{2x}\text{Se}_x$  [13, 14] and Cu atoms in tetrahedrite  $\text{Cu}_{12-x}\text{Tr}_x\text{Sb}_4\text{S}_{13}$  ( $\text{Tr} = \text{Mn}, \text{Fe}, \text{Co}, \text{Ni}, \text{Cu}, \text{and Zn}$ ) [15, 16]. This new type of rattling has extended the classes of materials in search of highperformance thermoelectric materials with small  $\kappa_L$  [13, 15–18].

The tetrahedrite crystallizes in a cubic structure with space group  $I\bar{4}3m$  as shown in the inset of Fig. 1 [19]. Note that the phase transition at 85 K accompanied by a structural transformation in pure tetrahedrite  $\text{Cu}_{12}\text{Sb}_4\text{S}_{13}$  [17, 20–26] is avoided by partial substitution

of  $Tr$  for Cu1 occupying a tetrahedron composed of four S1 atoms [17, 22]. The Cu2 atom is located in a triangle composed of two S1 atoms and one S2 atom, and has a large atomic displacement parameter (ADP) out of the  $S_3$  triangle and toward the Sb atoms for the cubic structure [16]. The low-energy quasi-localized vibrational mode of Cu2 has been revealed by neutron scattering measurements [17, 22, 27]. A systematic study of the crystal structure and phonon structure for  $Cu_{10}Zn_2Sb_4S_{13}$  (CZSS),  $Cu_{12}Sb_4S_{13}$  (CSS),  $Cu_{10}Zn_2As_4S_{13}$ , and  $Cu_{12}As_4S_{13}$  [27] demonstrated that the out-of-plane ADP for the Cu2 atom increases and simultaneously the characteristic energy of the out-of-plane vibration is reduced with decreasing the area of the  $S_3$  triangle. These results support the model that the rattling stems from the chemical pressure inherent in the triangle to squeeze the Cu2 atom out of the plane. On the other hand, based on the first-principles calculation, Lai *et al.* [28] have claimed that the rattling of the Cu2 atom in CSS is attributed to the creation of a covalent-type bonding between Cu and Sb through lone pairs of the trivalent Sb ion. Therefore, the driving mechanism of the rattling of the Cu2 atom in tetrahedrite has thus far remained an open question. If we measure the pressure effect on the rattling energy while keeping the chemical species (i.e. Sb or As) around the Cu2 atom intact, the dominant factor for the occurrence of rattling could be extracted. More specifically, it could be clarified how the rattling mode depends on the area of the  $S_3$  triangle and the Cu2-Sb distance.

The rattling mode in caged compounds manifests itself in a broad peak of the specific heat  $C$  divided by  $T^3$ , whose temperature is approximately 1/5 of the characteristic energy of rattling [29]. For both tetrahedrite CZSS and type-I clathrate BGS, a peak in  $C/T^3$  appears at 4 K, indicating the characteristic energy of the rattling mode to be 20 K [5, 9, 30].

In this Rapid Communication, we have compared the pressure dependences of the rattling modes for CZSS and BGS by specific heat measurements to shed light on the mechanism of the rattling in CZSS. We have found that application of pressures  $P$  up to 0.7 GPa reduces the rattling energy of CZSS but increases monotonically that of BGS. This opposite changes strongly indicate that the origin of anharmonicity in the rattling is different between CZSS with the planar coordination and BGS with the oversized cage. Upon further increasing  $P$  above 2.4 GPa, the rattling contribution to  $C/T^3$  for CZSS is fully suppressed, while the vibrational density of states in BGS at  $P = 6$  GPa remains more than 50% of that at  $P = 0$ . The cessation of rattling for  $P > 2.4$  GPa causes a profound change in the vibration of the

Cu atom from anharmonic rattling to a rather harmonic vibration in the local minimum of the potential out of the  $S_3$  triangle. The splitting of the Cu site is corroborated with synchrotron x-ray diffraction measurements under pressure.

Samples of polycrystalline  $\text{Cu}_{10}\text{Zn}_2\text{Sb}_4\text{S}_{13}$  (CZSS) and single-crystalline  $\text{Ba}_8\text{Ga}_{16}\text{Sn}_{30}$  (BGS) were synthesized in the manners as described elsewhere [5, 30]. The measurement of the specific heat  $C$  was performed by the ac method in pressure and temperature ranges of  $P \leq 6.5$  GPa and  $0.5 < T < 10$  K, respectively. Thereby, a Bridgman anvil cell was installed in a  $^3\text{He}$  cryostat [31]. The sample was wrapped in indium foil, which played the role of a pressure transmitting medium. The wrapped sample was packed in the cell by a gasket made of Cu–Be. The weights of the indium foil and gasket were 8.05 and 9.11 mg for CZSS (2.60 mg), and 9.52 and 9.09 mg for BGS (4.57 mg), respectively. Two chip resistors were used as the thermometer and the heater which were mounted on the outer flange of the gasket. Because the thermometer is free from pressure, it was not necessary to be calibrated under different pressures. The pressure was estimated by the pressure dependence of the superconducting transition temperature of the In foil. The details of the experimental set-up were described in Ref. [31]. The pressure dependence of the crystal structure of CZSS was examined at room temperature by synchrotron powder x-ray diffraction at the SPring-8, BL02B1 beamline. A pressure of up to 1.9 GPa was applied using a diamond anvil cell. By analyzing the diffraction patterns, we determined the atomic position and interatomic distances.

Figure 1 shows the temperature dependence of  $C/T^3$  for CZSS under various  $P$  up to 3.1 GPa. The data at  $P = 0$  with a broad maximum at 4 K agree with the previous data (open circles) measured by a Quantum Design physical property measurement system (PPMS) [30]. With increasing pressure up to 0.7 GPa, the value of  $C/T^3$  at around 2 K increases as a result of the shift of the broad maximum of  $C/T^3$  to low temperatures. Above 1 GPa, the  $C/T^3$  values at  $T > 2$  K decrease gradually, and for  $P \geq 2.4$  GPa, reach the value of the Debye specific heat with a Debye temperature of 242 K as shown by the dashed line [30]. Thus, the planar rattling mode of Cu2 is totally suppressed by the application of pressure.

The pressure effect on the planar rattling of Cu2 is very distinct from that on the rattling of Ba in a cage of BGS. The  $C/T^3$  data of BGS at  $P = 0$  show a broad maximum at 4 K, whose value agrees with that previously measured by PPMS (open circles) as shown in Fig. 2(a) [5, 9]. With increasing pressure up to 6.5 GPa, the broad maximum of  $C/T^3$

monotonically shifts to higher temperatures, maintaining a maximum value at a level more than half for  $P = 0$ . This result indicates the survival of the rattling of Ba with an increase in the characteristic energy.

Next, we turn our attention to the upturn of  $C/T^3$  observed at  $T < 1$  K for both CZSS and BGS. As shown in Fig. 1, the upturn for CZSS hardly changes with increasing pressure while that for BGS decreases drastically as shown in Fig. 2(a). This contrasting response implies distinct mechanisms of the upturn between the two systems. The upturn in BGS is due to the  $T$ -linear term of  $C(T)$  which originates from the quantum tunneling of the guest atom among off-center potential minima in the oversized cage [5, 9, 32]. Therefore, the reduction of  $C/T^3$  at  $T < 1$  K for BGS should be attributed to the pressure-induced change of the potential minimum from the off-center sites to the center in the cage. This interpretation is consistent with the Raman scattering study of rattling under pressure [10] and the chemical pressure effect on the specific heat [11, 32]. It was found that the  $T$ -linear specific heat of BGS is suppressed when the Sn atoms on the cage are replaced by Ge atoms with a smaller ionic radius [32]. On the contrary, the upturn of  $C/T^3$  for CZSS remains unchanged even at  $P \geq 2.4$  GPa, where the specific heat due to the rattling of Cu2 atoms is completely suppressed as discussed above. Therefore, the rattling of Cu2 atoms is not responsible for the upturn of  $C/T^3$ . We recall here that  $C(T)$  for  $T < 1$  K can be expressed by including a term proportional to  $T^{-\alpha}$  ( $\alpha > 1$ ) [30]. A similar behavior in cuprate superconductors was assigned to the Cu nuclear contribution as expressed by  $IT^{-2}$  [33]. Therefore, we fitted the specific heat data at  $T \leq 1$  K in terms of the form  $C(T) = IT^{-2} + \gamma T + \beta T^3$ , where  $\gamma T$  and  $\beta T^3$  represent the conduction-electron and Debye phonon contributions, respectively. Then, we calculated the phonon contribution  $\Delta C$  as  $\Delta C = C(T) - (IT^{-2} + \gamma T)$  for each pressure.

As shown in Fig. 2(b), the maximum temperature  $T_{\max}$  of  $\Delta C/T^3$  for CZSS initially decreases from 4 K for  $P = 0$  to 3.4 K at 0.7 GPa and slightly increases for  $P > 1$  GPa, while the maximum of  $C/T^3$  for BGS shifts to high temperatures monotonically as described above. In order to discuss quantitatively the pressure dependence of the vibrational density of states, we now analyze the specific heat data with the soft potential model (SPM) which could reproduce the broad maximum of  $C/T^3$  for clathrates [9, 29, 34]. This model assumes that the potential of the soft modes (SMs) for the rattler is given by  $V(x) = W(D_1 x + D_2 x^2 + x^4)$ , where  $W$  is the characteristic energy of the potential,  $x$  is the dimensionless displacement of the vibrating unit, and  $D_1$  and  $D_2$  are the coefficients of the asymmetry

and harmonic-potential terms which vary from mode to mode [35]. In addition to  $W$ , four parameters are used to fit the  $C(T)$ : the broadness of the SM,  $A$ ; the distribution constant of the SM,  $P_s$ ; the typical experimental time; and the minimum relaxation time [35]. This model assumes that the contributions from both the SM mode and tunneling mode (TM) of two-level systems increase at low temperatures [35]. As shown by the solid line in Fig. 2(b), the broad maximum of the  $\Delta C/T^3$  of CZSS at  $P = 0$  was reproduced with the parameters  $A = 0.045$ ,  $W/k_B = 4.0$  K, and  $P_s = 5.9 \times 10^{21} \text{ mol}^{-1}$ , without including the contribution of the TM. The data for BGS at  $P = 0$  were fit with the parameters  $A = 0.017$ ,  $W/k_B = 3.5$  K, and  $P_s = 6.7 \times 10^{21} \text{ mol}^{-1}$ , which agree with previously reported values [9]. The data of  $\Delta C/T^3$  of CZSS at low pressures and above 5 K could not be reproduced by the SPM. This discrepancy may be attributed to the fact that the phenomenological SPM model does not take into account the vibrational modes at a higher energy compared with the rattling energy.

Figures 2 (c) and 2(d) show, respectively, the vibrational density of states  $g(\nu)/\nu^2$  for BGS and CZSS under various pressures as a function of the frequency  $\nu$  used for the fit with the SPM model. The pressure dependences of  $\nu_{\text{max}}$  and the maximal values of  $g(\nu)/\nu^2$  at  $\nu = \nu_{\text{max}}$  are displayed in Figs. 3(a)-(d). For BGS, the monotonic increase of  $\nu_{\text{max}}$  with increasing pressure suggests a gradual increment of harmonicity in the vibration of the Ba guest atom in the cage. A similar increase in the rattling energy for  $\text{Sr}_8\text{Ga}_{16}\text{Ge}_{30}$  was observed when the cage was shrunk by the substitution of Si for Ge [11]. For CZSS, the frequency at the peak  $\nu_{\text{max}} = 0.4$  THz corresponds to the rattling energy of 1.7 meV, which is between the two characteristic energies 1.0 and 2.8 meV obtained by an analysis of the specific heat with the Einstein model [36]. The reduction in  $\nu_{\text{max}}$  up to 0.7 GPa for CZSS shown in Fig. 3(c) indicates the enhancement of anharmonicity in the vibration of the Cu2 atom. This result is reproduced by the soft-mode dynamic theory considering the interaction between the acoustic phonon and soft-mode vibrational excitations [37]. The opposite  $P$  dependences indicate that origins of anharmonicity are distinct between the out-of-plane rattling of Cu2 atoms in CZSS and the rattling of Ba ions in the cage of BGS. On further increasing pressure to  $P > 1$  GPa, the value of  $\nu_{\text{max}}$  for CZSS increases steeply. This fact suggests the enhancement of harmonicity in the vibration of Cu2 atoms. It is noteworthy that the value of  $g(\nu)/\nu^2(\text{max})$  for CZSS decreases with further increasing  $P$  as shown in Fig. 3 (d). The additional contribution of SM over the Debye phonon contribution (dashed line)

disappears for  $P > 2.4$  GPa. The cessation of the vibrational density of states is in contrast with the case of BGS shown in Fig. 3(b), where  $g(\nu)/\nu^2(\text{max})$  levels off at around 4 GPa but remains at half of the initial value even at 6 GPa. The very different  $P$  dependence indicates that the planar rattling of Cu2 atoms in CZSS is more fragile to pressure than the rattling of Ba atoms in the cage of BGS.

Table I shows the structural parameters for CZSS under pressures of 0.3 and 1.9 GPa at room temperature. We analyzed the powder x-ray diffraction patterns by using an on-site model and a split-site model. The on-site model assumes that atoms are located at the crystallographic sites in the cubic structure ( $I\bar{4}3m$ ): Cu1 at  $12d$  ( $1/2, 0, 1/4$ ), Cu2 at  $12e$  ( $0, 0, z$ ), Sb at  $8c$  ( $x, x, x$ ), S1 at  $24g$  ( $x, x, z$ ), and S2 at  $2a$  ( $0, 0, 0$ ) [16, 18, 19, 24–28]. In the split-site model, the site for Cu2 splits into a  $24g$  site (Cu22) out of the  $S_3$  triangle and the original  $12e$  site (Cu21) [19], and simultaneously the site of S2 splits into a  $12e$  site (S22) and the original  $2a$  site (S21). Occupancies and shifts of additional sites in the split-site model were almost zero in the refinement of the 0.3 GPa diffraction pattern. The x-ray diffraction pattern was well reproduced by the on-site model. This result is consistent with previous refinements of the diffraction data at ambient pressure using the two models [25, 27]. On the contrary, the Rietveld refinement of the pattern at 1.9 GPa with the split-site model gave reliability factors of Bragg intensities,  $R_I = 5.088\%$ , and the weighted profile,  $R_{wp} = 1.282\%$ , whose values are, respectively, smaller than those of the refinement with the on-site model ( $R_I = 5.224\%$ ,  $R_{wp} = 1.338\%$ ). This means that the Cu2 atom at 1.9 GPa has a large probability to be located at the local potential minimum out of the  $S_3$  triangle.

Based on the structural parameters for CZSS, we discuss the change in the rattling energy of the Cu2 atom upon applying pressure up to 0.7 GPa. As shown in Fig. 3(c), the rattling energy of  $\nu_{\text{max}}$  for CZSS decreases by 14% from 0.37 THz at 0 GPa to 0.32 THz at 0.7 GPa. At first, we focus on the role of lone pairs of Sb for the rattling of the Cu2 atom. Lai *et al.* claimed that covalent-type “out-of-plane bonding” between Cu2 and Sb via the lone pairs leads to a rattling of Cu2 [28]. The Cu2-Sb distance,  $d(\text{Cu2-Sb})$ , is a measure of the free space for the out-of-plane vibration of Cu2 as well as that of the magnitude of electron sharing between Cu2 and Sb. The decreasing ratio of  $d(\text{Cu2, Cu21-Sb})$  upon pressurizing from 0.3 to 1.9 GPa is estimated to be  $0.029 \text{ \AA/GPa}$  using the values listed in Table I. This ratio gives a reduction in  $d(\text{Cu2-Sb})$  of  $0.02 \text{ \AA}$  upon pressurizing from  $P = 0$  to 0.7 GPa. This value is only 0.6% for  $d(\text{Cu21-Sb}) = 3.344 \text{ \AA}$  [27]. The small change in



$d(\text{Cu2-Sb})$  suggests a weak and positive correlation between  $\nu_{\text{max}}$  and  $d(\text{Cu2-Sb})$ . On the contrary, a negative correlation was reported for the substituted system of CSS [27]. In fact, the rattling energy  $E_{\text{R}}$  of Cu2 decreases by 19% ( $\nu_{\text{max}}$  by 14%) by the substitution of As for Sb in CSS [27], where  $d(\text{Cu2-As})$  is elongated compared to  $d(\text{Cu2-Sb})$ . These comparisons of the pressure effect with the substitution effect indicate the minor role of lone pairs in the rattling of the Cu2 atom.

In turn, we discuss the relationship between  $E_{\text{R}}$  of the Cu2 atom and the  $S_3$  triangle area  $S_{\text{tri}}$ . It was reported that  $E_{\text{R}}$  decreases with decreasing  $S_{\text{tri}}$  on going from CZSS, CSS,  $\text{Cu}_{10}\text{Zn}_2\text{As}_4\text{S}_{13}$ , to  $\text{Cu}_{12}\text{As}_4\text{S}_{13}$  [27]. Let us compare the pressure effect on  $E_{\text{R}}$  with the substitution effect. As shown in Table I, the average value of  $6.07(3) \text{ \AA}^2$  of  $S_{\text{tri}}$  at  $P = 1.9$  GPa is 3.5% smaller than that for  $P = 0.3$  GPa. Therefore, the decreasing ratio of  $S_{\text{tri}}$  is 2.2 %/GPa. From Fig. 3(c), the decreasing ratio of the rattling energy of  $\nu_{\text{max}}$  is 20%/GPa in the  $P$  range from 0 to 0.7 GPa. These values yield  $d(\ln\nu_{\text{max}})/d(\ln S_{\text{tri}}) = 9$ , which agrees with  $d(\ln E_{\text{R}})/d(\ln S_{\text{tri}})$ . The latter was estimated from the analysis for the substituted systems CZSS, CSS,  $\text{Cu}_{10}\text{Zn}_2\text{As}_4\text{S}_{13}$ , and  $\text{Cu}_{12}\text{As}_4\text{S}_{13}$  [27]. This agreement indicates that  $S_{\text{tri}}$  is the dominant parameter that controls the rattling of the Cu2 atom in CZSS. Thus, it is proved that the rattling in CZSS originates from the chemical pressure inherent in the  $S_3$  triangle to squeeze the Cu2 atom out of the plane.

We now turn to a discussion of the vibrational state of the Cu2 atom in CZSS for the range  $P > 1$  GPa. As shown in Figs. 2(d) and 3(d), the density of states for the rattling of the Cu2 atom decreases strongly for  $P > 1$  GPa and disappears for  $P > 2.4$  GPa. Furthermore, as presented in Fig. 3(c), the rattling energy  $\nu_{\text{max}}$  increases for  $P > 1$  GPa, indicative of the enhancement of harmonicity in the vibration of the Cu2 atom. As shown in Table I, the distance between Cu22 and Sb is  $2.49(6) \text{ \AA}$  at 1.9 GPa, which is close to the distance of  $2.2 \text{ \AA}$  between Cu21 and S. Thereby, the bond order value of about 0.5 for the Cu22-Sb pair becomes five times larger than that for the Cu21-Sb pair reported in Ref. 28. These facts allow us to speculate that the Cu2 atom is ejected from the  $S_3$  plane due to the chemical pressure, and is combined with Sb for  $P > 2$  GPa. This scenario is consistent with the suppression of the vibrational density of states for the rattling of Cu2 atoms.

In summary, we have studied the pressure effect on the rattling mode in tetrahedrite  $\text{Cu}_{10}\text{Zn}_2\text{Sb}_4\text{S}_{13}$  (CZSS) and type-I clathrate  $\text{Ba}_8\text{Ga}_{16}\text{Sn}_{30}$  (BGS) by specific heat measurements up to 6 GPa. For  $P = 0$ , the  $C/T^3$  data for both systems exhibit a maximum at 4 K,



five times of which is a measure of the rattling energy. With increasing pressure, the energy for CZSS initially decreases and steeply increases for  $P > 1$  GPa while that for BGS increases monotonically. Furthermore, the upturn of  $C/T^3$  at  $T < 1$  K for CZSS hardly changes with increasing pressure while that for BGS decreases drastically. These contrasting responses of  $C/T^3$  are attributed to distinct mechanisms for the rattling between the two systems. For the Ba guest ions in an oversized cage of BGS, an application of pressure shifts the potential minimum from the off-center sites to the center in the cage, and thus increases the harmonicity in the vibration of Ba ions.

For CZSS, the synchrotron powder x-ray diffraction measurement has revealed that the area of  $S_3$  triangle, the  $S_{\text{tri}}$ , decreases with increasing pressure up to 1.9 GPa. The systematic dependences of the rattling energy on  $S_{\text{tri}}$  by an application of pressures and substitutions strongly indicate that the dominant parameter controlling the rattling of the Cu2 atom in CZSS is not the distance  $d(\text{Cu2-Sb})$  but the area  $S_{\text{tri}}$ . These findings support that the rattling in CZSS originates from the chemical pressure inherent in the triangle to squeeze the Cu2 atom out of the plane. On further increasing pressure up to 2.4 GPa, the specific heat due to the rattling modes completely disappears. This is consistent with the splitting of the Cu2 site as indicated by the x-ray diffraction analysis on the data at 1.9 GPa. At  $P > 2$  GPa, the Cu2 atom is likely to vibrate near the local potential minimum out of the  $S_3$  triangle.

Our study verified high-pressure specific heat measurement as a strong tool to investigate the rattling modes in solids. Furthermore, the pressure-sensitive planar rattling modes found in tetrahedrite would allow us to provide different guidelines for the development of high-performance thermoelectric materials.

We acknowledge valuable discussions with C. H. Lee and T. Onimaru. The specific heat measurement under pressures were performed at N-BARD, Hiroshima University. This work was partly supported by Japan Society for the Promotion of Science KAKENHI Grants No. JP25400375, No. JP16H01073, No. JP18K03518, No. JP18H04324, No. JP18H04499, and CREST JST Grants No. JPMJCR16Q6, and No. JPMJCR20Q4. Synchrotron radiation x-ray diffraction experiments were carried out at SPring-8 with the approval of the Japan Synchrotron Radiation Research Institute (Proposals No. 2018B0078 and No. 2019A0159).

---

\* e-mail address: kumeo@hiroshima-u.ac.jp

- [1] V. Keppens, D. Mandrus, B. C. Sales, B. C. Chakoumakos, P. Dai, R. Coldea, M. B. Maple, D. A. Gajewski, E. J. Freeman, and S. Bennington, *Nature* **395**, 876 (1998).
- [2] T. Takabatake, K. Suekuni, T. Nakayama, E. Kaneshita, *Rev. Mod. Phys.* **86**, 669 (2014) and references therein.
- [3] G. A. Slack, in *CRC Handbook of Thermoelectrics*, edited by M. Rowe (CRC Press, Boca Raton, FL, 1995), p. 407.
- [4] B. C. Sales, B. C. Chakoumakos, R. Jin, J. R. Thompson, and D. Mandrus, *Phys. Rev. B* **63**, 245113 (2001).
- [5] M. A. Avila, K. Suekuni, K. Umeo, H. Fukuoka, S. Yamanaka, and T. Takabatake, *Appl. Phys. Lett.* **92**, 041901 (2008).
- [6] Y. Nagao, J. I. Yamaura, H. Ogusu, Y. Okamoto, and Z. Hiroi, *J. Phys. Soc. Jpn.* **78**, 064702 (2009).
- [7] D. J. Sarik, T. Klimczuk, A. Llobet, D. D. Byler, J. C. Lashley, J. R. O'Brien, and N. R. Dilley, *Phys. Rev. B* **85**, 014103 (2012).
- [8] T. Tadano, and S. Tsuneyuki, *Phys. Rev. Lett.* **120**, 105901 (2018)
- [9] K. Suekuni, M. A. Avila, K. Umeo, H. Fukuoka, S. Yamanaka, T. Nakagawa, and T. Takabatake, *Phys. Rev. B* **77**, 235119 (2008).
- [10] T. Sukemura, T. Kume, T. Matsuoka, S. Sasaki, T. Onimaru, and T. Takabatake, *J. Phys.: Conference Series* **500**, 182022 (2014).
- [11] K. Suekuni, M. A. Avila, K. Umeo, and T. Takabatake, *Phys. Rev. B* **75**, 195210 (2007).
- [12] C. H. Lee, *J. Phys. Soc. Jpn.* **88**, 041009 (2019).
- [13] A. Nishida, O. Miura, C. H. Lee, Y. Mizuguchi, *Appl. Phys. Express* **8**, 111801 (2015).
- [14] Y. Mizuguchi, A. Miura, A. Nishida, O. Miura, K. Tadanaga, N. Kumada, C. H. Lee, E. Magome, C. Moriyoshi, Y. Kuroiwa, *J. Appl. Phys.* **119**, 155103 (2016).
- [15] X. Lu, D. T. Morelli, Y. Xia, F. Zhou, V. Ozolins, H. Chi, X. Zhou, and C. Uher, *Adv. Energy Mater.* **3**, 342 (2013).
- [16] K. Suekuni, K. Tsuruta, M. Kunii, H. Nishiate, E. Nishibori, S. Maki, M. Ohta, A. Yamamoto, and M. Koyano, *J. Appl. Phys.* **113**, 043712, (2013).

- [17] K. Suekuni, K. Tsuruta, T. Ariga, and M. Koyano, *Appl. Phys. Express* **5**, 051201 (2012).
- [18] Y. Bouyrie, C. Candolfi, S. Pailh  s, M. M. Koza, B. Malaman, A. Dauscher, J. Tobola, O. Boisson, L. Saviote, and B. Lenoira, *Phys. Chem. Chem. Phys.* **17**, 19751 (2015).
- [19] A. Pfitzner, M. Evain, and V. Petricek, *Acta Cryst.* **B53**, 337 (1997).
- [20] S. Kitagawa, T. Sekiya, S. Araki, T. C. Kobayashi, K. Ishida, T. Kambe, T. Kimura, N. Nishimoto, K. Kudo, and M. Nohara, *J. Phys. Soc. Jpn.* **84**, 093701 (2015).
- [21] H. I. Tanaka, K. Suekuni, K. Umeo, T. Nagasaki, H. Sato, G. Kutluk, E. Nishibori, H. Kasai, and T. Takabatake, *J. Phys. Soc. Jpn.* **85**, 014703 (2016).
- [22] A. F. May, O. Delaire, J. L. Niedziela, E. Lara-Curzio, M. A. Susner, D. L. Abernathy, M. Kirkham, and M. A. McGuire, *Phys. Rev. B* **93**, 064104 (2016).
- [23] D. I. Nasonova, V. Yu. Verchenko, A. A. Tsirlin, and A. V. Shevelkov, *Chem. Mater.* **28**, 6621 (2016).
- [24] N. Ghassemi, X. Lu, Y. Tian, E. Conant, Y. Yan, X. Zhou, and J. H. Ross, Jr., *ACS Appl. Mater. Interfaces* **10**, 36010 (2018).
- [25] V. R. Hathwar, A. Nakamura, H. Kasai, K. Suekuni, H. I. Tanaka, T. Takabatake, B. B. Iversen, and E. Nishibori, *Cryst. Growth Des.* **19**, 3979 (2019).
- [26] S. O. Long, A. V. Powell, S. Hull, F. Orlandi, C. C. Tang, A. R. Supka, M. Fornari, and P. Vaqueiro, *Adv. Funct. Mater.* **30**, 1909409 (2020).
- [27] K. Suekuni, C. H. Lee, H. I. Tanaka, E. Nishibori, A. Nakamura, H. Kasai, H. Mori, H. Usui, M. Ochi, T. Hasegawa, M. Nakamura, S. Ohira-Kawamura, T. Kikuchi, K. Kaneko, H. Nishiate, K. Hashikuni, Y. Kosaka, K. Kuroki, and T. Takabatake, *Adv. Mater.* 1706230 (2018).
- [28] W. Lai, Y. Wang, D. T. Morelli, and X. Lu, *Adv. Funct. Mater.* **25**, 3648 (2015).
- [29] L. Gil, M. A. Ramos, A. Bringer, and U. Buchenau, *Phys. Rev. Lett.* **70**, 182 (1993).
- [30] K. Suekuni, H. I. Tanaka, F. S. Kim, K. Umeo, and T. Takabatake, *J. Phys. Soc. Jpn.* **84**, 103601 (2015).
- [31] K. Umeo, *Rev. Sci. Instrum.* **87**, 063901 (2016).
- [32] J. Wu, J. Xu, D. Prananto, H. Shimotani, Y. Tanabe, S. Heguri, and K. Tanigaki, *Phys. Rev. B* **89**, 214301 (2014).
- [33] N. Wada, H. Muro-oka, Y. Nakamura, and K. Kumagai, *Physica C* **157**, 453 (1989).
- [34] K. Umeo, M. A. Avila, T. Sakata, K. Suekuni, and T. Takabatake, *J. Phys. Soc. Jpn.* **74**,

2145 (2005).

- [35] M. A. Ramos and U. Buchenau: in *Tunneling Systems in Amorphous and Crystalline Solids*, ed. P. Esquinazi (Springer, Berlin, 1998) Chap. 9, p. 527.
- [36] E. Lara-Curzio, A. F. May, O. Delaire, M. A. McGuire, X. Lu, Cheng-Yun Liu, E. D. Case, and D. T. Morelli, *J. Appl. Phys.* **115**, 193515 (2014).
- [37] M. Baggioli, B. Cui, and A. Zaccone, *Phys. Rev. B* **100**, 220201(R) (2019).

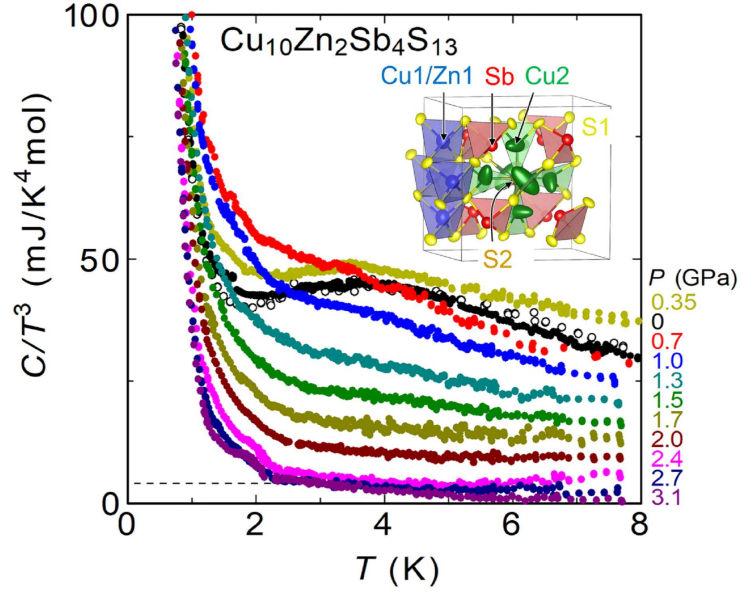


FIG. 1. Temperature dependence of the specific heat  $C$  divided by  $T^3$ ,  $C/T^3$ , for  $\text{Cu}_{10}\text{Zn}_2\text{Sb}_4\text{S}_{13}$  under various constant pressures up to 3.1 GPa. The data for  $P = 0$  (solid black circles) agree with the previous data (open black circles) measured by Quantum Design PPMS [30]. The dashed line at the bottom represents the calculation using the Debye model with a Debye temperature of 242 K [30].

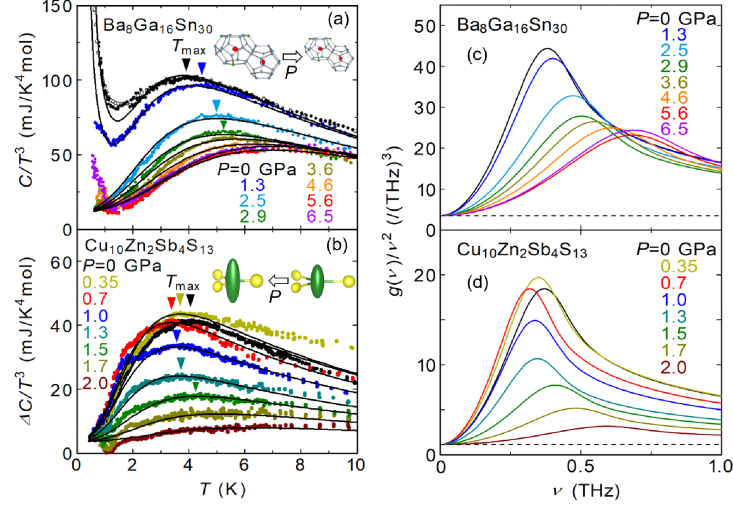


FIG. 2. (a) Specific heat  $C$  divided by  $T^3$ ,  $C/T^3$  vs  $T$  for  $\text{Ba}_8\text{Ga}_{16}\text{Sn}_{30}$  (BGS) up to 6.5 GPa, and (b) the lattice contribution of  $C/T^3$ ,  $\Delta C/T^3$ , vs  $T$  for  $\text{Cu}_{10}\text{Zn}_2\text{Sb}_4\text{S}_{13}$  (CZSS) under pressures up to 2 GPa. Solid lines are fits using the soft potential model (SPM). The shoulders in  $\Delta C/T^3$  near 2 K for CZSS are experimental artifacts caused by no smooth connection of calibration curves of the thermometer used for the specific heat measurements. The vibrational density of states  $g(\nu)/\nu^2$  calculated by SPM for (c) BGS and (d) CZSS as a function of frequency  $\nu$ . The dashed lines represent calculations using the Debye model with Debye temperatures of 210 K [9] and 242 K [30] for BGS and CZSS, respectively.

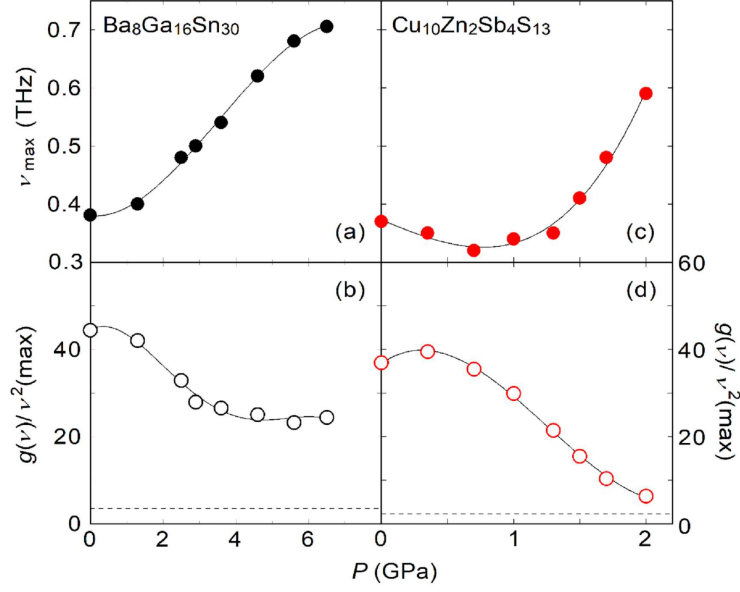


FIG. 3. Pressure dependences of the frequency  $\nu_{\max}$  at which the vibrational density of states  $g(\nu)/\nu^2$  in Figs. 2(c) and 2(d) has the maximum, and a maximal value of  $g(\nu)/\nu^2$  for  $\text{Ba}_8\text{Ga}_{16}\text{Sn}_{30}$  [(a), (b)] and  $\text{Cu}_{10}\text{Zn}_2\text{Sb}_4\text{S}_{13}$  [(c), (d)]. Solid lines are guides for the eyes. The dashed lines in (b) and (d) represent calculations using the Debye model with Debye temperatures of 210 K [9] and 242 K [30] for BGS and CZSS, respectively.



TABLE I. Crystallographic parameters of  $\text{Cu}_{10}\text{Zn}_2\text{Sb}_4\text{S}_{13}$  for  $P = 0.3$  and 1.9 GPa at 300 K: Lattice constant, atomic coordination, occupancy, interatomic distances, and area of  $\text{S}_3$  triangle,  $S_{\text{tri}}$ .

Parameter	0.3 GPa (onsite)	1.9 GPa (split site)
$a$ (Å)	10.3429 (3)	10.2607 (3)
$R_{\text{wp}}$ (%)	1.142	1.282
$R_{\text{I}}$ (%)	3.769	5.088
Cu1 in $12d(1/2, 0, 1/4)$ ; occ.	2/3	2/3
Zn1 in $12d(1/2, 0, 1/4)$ ; occ.	1/3	1/3
Cu2 in $12e(0, 0, z)$ ; occ.	$z = 0.2167$ ; 1.0	—
Cu21 in $12e(0, 0, z)$ ; occ.	—	$z = 0.2172$ (6); 0.85
Cu22 in $24g(x, -x, z)$ ; occ.	—	$x = 0.061$ (5), $z = 0.191$ (4); 0.075
S1 in $24g(x, x, z)$ ; occ.	$x = 0.1141$ (5), $z = 0.3644$ (4); 1.0	$x = 0.1115$ (7), $z = 0.3646$ (5); 1.0
S2 in $2a(0, 0, 0)$ ; occ.	1.0	—
S21 in $2a(0, 0, 0)$ ; occ.	—	0.15
S22 in $12e(x, 0, 0)$ ; occ.	—	$x = 0.058$ (3); 0.1417
Sb in $8c(x, x, x)$ ; occ.	$x = 0.2684$ (3); 1.0	$x = 0.2697$ (4); 1.0
$d(\text{Cu2-Sb})$ (Å)	3.391 (3)	—
$d(\text{Cu21-Sb})$ (Å)	—	3.344 (5)
$d(\text{Cu22-Sb})$ (Å)	—	2.49 (6)
$d(\text{S1-S1})$ (Å)	3.337 (11)	3.235 (15)
$d(\text{S1-S2})$ (Å)	4.121 (5)	—
$d(\text{S1-S21}), d(\text{S1-S22})$ (Å)	—	4.075 (6), 3.54 (4), 3.950 (8), 4.279 (16), 4.62 (4)
$S_{\text{tri}}$ (Å <sup>2</sup> )	6.29 (3)	6.05 (4), 5.09 (12), 6.09 (5), 7.00 (16); Ave., 6.07 (3)